Soft fluorescent organic nanodots as nanocarriers for porphyrins

Isabelle Sasaki, Jonathan Daniel, Sebastien Marais, Jean-Baptiste Verlhac, Michel Vaultier, Mireille Blanchard-desce

Soft fluorescent organic nanodots as nanocarriers for porphyrins

Isabelle Sasaki,[a] Jonathan Daniel,[a] Sébastien Marais,[b] Jean-Baptiste Verlhac,[a] Michel Vaultier[a] and Mireille Blanchard-Desce[a]*

[a)] Univ. Bordeaux, Institut des Sciences Moléculaires, (CNRS UMR5255), Bâtiment A12, 351 Cours de la Libération, 33405 TALENCE CEDEX, France.

[b)] CNRS, Univ. Bordeaux, Bordeaux Imaging Center, UMS 3420, 33000 Bordeaux, France

Received date (to be automatically inserted after your manuscript is submitted)

Accepted date (to be automatically inserted after your manuscript is accepted)

ABSTRACT: Novel fluorescent organic nanoparticles made from citric acid and diethylenetriamine were used as biocompatible and highly water-soluble nanocarriers for hydrophobic tetraphenylporphyrin (**TPP**). The tetraphenylporphyrin units were covalently attached to the nanoparticles, generating conjugated nanoparticles which retain water solubility and preserve the photophysical properties of monomeric **TPP**. The conjugated nanoparticles show two distinct fluorescence features: blue emission from the nanoparticle when excited in the near UV (360 nm) and characteristic far-red emission of the **TPP** when excited in the visible (Soret band or Q bands). The uptake of the conjugated nanoparticles in live human neuroblastoma cancer cells was evidenced using two-photon microscopy. These experiments demonstrate that the fluorescence organic nanoparticles do act as efficient nanocarriers allowing the cell internalization of the hydrophobic porphyrins. These conjugated nanoparticles appear as promising nanotools for theranostic based on the combination of imaging (monitoring of the nanoparticle fluorescence) and therapeutic (photodynamic therapy by selectively exciting the grafted porphyrin units) modalities.

KEYWORDS: Porphyrins, Water-solubility, Fluorescence, Nanocarrier, Two-photon imaging

* Correspondence to: Mireille Blanchard-Desce, Université de Bordeaux, Institut des Sciences Moléculaires, Bat A12, 351 Cours de la Libération, 33405 Talence cedex, France, Tel+33 540006731, E-mail : mireille.blanchard-desce@u-bordeaux.fr.

INTRODUCTION

The development of new approaches for cancer therapy is one of the most important challenges of medicine in the 21st century, in line with a steep increase in the occurrence of oncological diseases in the last decades. Latest global cancer data indicate that the incidence of cancer attains 18.1 million new cases and 9.6 million cancer deaths in 2018. Among various therapies used in oncology, photodynamic therapy (PDT)[1,2] appears as a promising alternative or adjuvant treatment to surgery, chemotherapy or radiotherapy. PDT is particularly interesting with respect to the relapse issue as cells are generally unable to develop resistance. PDT requires the use of photosensitizers (PS) which cause cell death by necrosis and/or apoptosis only under appropriate illumination. When excited by light, the PS generates reactive oxygen species (including singlet oxygen) that induce damages of the cell and subsequent cell death. Among various PS, porphyrin derivatives, such as porfimer sodium (Photofrin®) and verteporfin (Visudyne®) are used in clinics. These exhibit high singlet oxygen quantum yields and reduced toxicity in the absence of light. However, porphyrins such as tetraphenylporphyrin (**TPP**) which shows both fluorescence and high singlet oxygen generation quantum yields in low polarity organic solvents are markedly hydrophobic [3]. The addition of water-solubilizing charged side groups (such as carboxylate, sulfonate …) improve their water-solubility but may also lead to self-aggregation which can be deleterious to both fluorescence and singlet oxygen generation. In that perspective, the use of nanocarriers that improve the bioavailability of drugs is of major interest. In recent years, a wide range of nanotechnology-based drug delivery systems have been developed in order to improve the solubility, bioavailability and efficiency of chemotherapeutic drugs [4,5]. These include liposomes [6], polymeric micelles [7], nanoemulsions [8], polymeric nanoparticles [9], dendrimers [10], gold nanoparticles [11], carbon dots [12], etc. In that respect, the encapsulation of porphyrins in micelles was demonstrated to prevent self-aggregation induced fluorescence quenching [13].

The use of nanoparticles made of natural components (proteins [14], peptides [15], carbohydrates [16]...) as nanocarriers represents an attractive approach in relation with their biocompatibility. As an example, nanoparticles made of albumin are used in clinics for formulating paclitaxel, a highly hydrophobic anticancer drug [17]. In this framework, we have been interested in using novel soft organic nanodots made from citric acid and diethylenetriamine as biocompatible and fluorescent water-soluble nanocarriers. These soft fluorescent organic nanoparticles (**FONPs**) show high water solubility (>250 g/L), bright blue fluorescence in aqueous media as well as large two-photon absorption in the 700-750 nm range which is interest for bioimaging [18]. Furthermore, these **FONPs** were recently demonstrated to show in vitro safety and preferential internalization in glioblastoma cells. These **FONPs** were successfully used as drug delivery systems for paclitaxel (**PTX**). **PTX-conjugated FONPs** retain excellent solubility in water and remain stable in water while they showed anticancer activity against glioblastoma cells in 2D and 3D culture [18]. As such, **FONPs** hold major promises for nanomedecine, in particular for cancer treatment. Following this route, we thus investigated the potential of **FONPs** as nanocarrier for porphyrins aiming at designing novel water-soluble PS for PDT.

RESULTS AND DISCUSSION

Synthesis and characterization of the conjugated FONPs[TPP]

The synthetic pathway to **FONPs[TPP]** involve 3 steps (Scheme 1). Firstly (scheme 1, step 1), **FONPs** were prepared via a bottom-up synthesis by polycondensation of an equimolar mixture of citric acid and diethylenetriamine (**DETA**). These **FONPs** show very high water-solubility due to the presence of numerous carboxylic acid (COOH) and amine functions [18]. In the second step, the **FONPs** were activated by treatment with a large excess of ethylenediamine in order to achieve surface functionalization with a large number of free accessible NH_2 moieties (scheme 1, step 2). These surface NH_2 groups can subsequently be used to covalently attach different bioactive molecules via various bioconjugation reactions. By reacting the activated **FONPs** with tetraphenylporphyrine isothiocyanate (**TPP-ITC**) for 16 hours in DMSO (scheme 1, step 3), covalent grafting of the tetraphenylporphyrine (**TPP**) on the **FONPs** could be achieved. The unreacted **TPP-ITC** was eliminated by washing with dichloromethane and the resulting **FONPs[TPP]** were obtained as a brown powder.

<Scheme 1>

<Fig. 1>

The nanoparticles were characterized by transmission electron microscopy (TEM). As shown in Fig. 1, both the nanocarriers (**FONPs-NH_2**) and the **FONPs[TPP]** show a small diameter (10 nm) which remains unaffected by the grafting of the **TPP** units. The grafting of the porphyrins was demonstrated by UV-vis absorption (Fig. 2). The characteristic Soret band of the porphyrins is clearly observed at 420 nm, overlapping with the tail of the near-UV absorption band of the **FONPs**. The less intense four Q bands are also clearly noticeable at 520, 555, 590, 650 nm (see inset in Fig. 1). These characteristic absorption bands allowed the determination of the amount of grafted porphyrins, yielding a value of 50 μmoles of grafted **TPP** units per gram of **FONPs[TPP]**. Interestingly, the **FONPs[TPP]** retain good solubility in water and show positive ζ-potential (51 mV), indicative of a large number of NH_3^+ surface groups. This positive surface potential is of high relevance with respect to cell internalization. Recently enhanced cellular penetration was observed with porphyrins bearing cationic charges [19].

<Fig. 2>

Fluorescence properties

The fluorescence properties of the **FONPs[TPP]** were investigated in pure water (Table 1). As noted from Fig. 3, the **FONPs[TPP]** retain the fluorescence properties of both the **FONPs** nanocarrier and of the grafted porphyrins. When excited in the near UV (360 nm), a blue fluorescence with emission spectra peaking at 460 nm is observed (Fig. 3A). This fluorescence originates from the **FONPs** nanocarrier as clearly evidenced in the corresponding excitation spectrum (Fig.3B). In contrast, the far red emission of **TPP** is observed upon excitation in the Q bands (Fig. 3A). We note that the corresponding excitation spectrum (Fig.3B) is similar to that of **TPP** dissolved in toluene indicating that the **TPP** do not aggregate in the conjugated nanoparticles.

<Table 1>

<Fig. 3>

FONPs[TPP] are thus two-color nanoparticles which can be excited either (i) at 360 nm to generate the blue fluorescence of the platform (Fig. 3B) or (ii) in the Soret band (>430 nm) or in the Q bands to excite selectively the **TPP** units (Fig. 3B). This is of major promise for theranostics applications as selective excitation of the **FONPs** could potentially allow tracking of the nanocarriers without exciting the porphyrins (imaging modality) while selective excitation of the **TPP** could be used for the therapy modality (PDT).

Internalization of FONPs[TPP] in human neuroblastoma cells line

The ability of **FONPs[TPP]** to penetrate into cancer cells vas investigated using BE(2)-M17 cells line. The uptake of the nanoparticles was monitored using two-photon excited fluorescence (TPEF) imaging. Compared to confocal fluorescence imaging, TPEF bioimaging allows improved penetration in tissues, intrinsic three-dimensional resolution and reduction of background fluorescence. We previously reported that **FONPs** show large two-photon absorption responses in the 700-750 nm range with maximum two-photon absorption cross-section (σ_2^{max}) of 7000 GM at 730 nm [18]. In contrast, **TPP** show moderate two-photon absorption with σ_2 value of 18 GM at 790 nm [20] but the substantial number of porphyrins grafted on the nanoparticles should lead to a large two-photon absorption cross-section value for the **FONPs[TPP]** at this wavelength.

<Fig. 4>

We thus performed two-photon imaging at the two different wavelengths to assess the uptake of the nanoparticles and porphyrins. As shown in Fig. 4, the uptake of **TPP** is clearly demonstrated by monitoring the far-red fluorescence of TPP upon two-photon excitation at 790 nm. On the other hand, when exciting at 730 nm, the uptake of the nanoparticles is clearly observable by monitoring only the blue fluorescence of the **FONPs** in the 400-550 nm range (Fig. 5).

<Fig. 5>

These imaging experiments demonstrate that the **TPP**-conjugated **FONPs** are internalized into BE(2)-M17 human cancer cells and that the **FONPs** do act as nanocarriers allowing efficient uptake of **TPP** into the cancer cells. These results open a new route towards novel biocompatible nanoparticle for PDT and theranostics. In particular by grafting of NIR fluorescent dyes and targeting agents [21], multifunctional nanoparticles for both *in vitro* and *in vivo* imaging as well as two-photon photodynamic therapy would be achievable. We are currently exploring this route.

EXPERIMENTAL

Synthesis

General

The starting materials were purchased from Aldrich, TCI and Alfa Aesar. 5-(4-aminophenyl)-l0,15,20-triphenylporphyrine (TPP-NH_2) was prepared as previously reported [22]. Reactions were monitored by thin layer chromatography on Merck silica gel 60F254 pre-coated aluminum sheets. Column chromatography was performed on Fluka silica gel 60 (40-63 μm). 1H NMR spectra were recorded on Bruker AVANCE I 300spectrometer. Chemical shifts are given in parts per million with respect to residual solvent peak and coupling constant (J) are given in Hertz.

Synthesis and activation of fluorescent organic nanoparticles

Diethylenetriamine (1.35 mL, 13.7 mmol) was added dropwise to a solution of citric acid (2.62 g, 13.6 mmol) in distilled water (10 mL). After water evaporation, the residue was heated at 200°C for 30 min leading to a brown resin. Ethylenediamine (15 mL) was added to the residue and the reaction mixture was boiled for 12 hours. Unreacted excess of ethylenediamine was removed by evaporation under vacuum. Ethanol was added to the brown residue. A light-brown powder was isolated by centrifugation (10 000 rpm for 10 min), washed twice with diethyl ether, dried under vacuum and

yielding a first crop of light-brown solid (480 mg). A second crop was collected by centrifugation (followed by washing and drying) after flocculation of the ethanolic filtrate upon addition of diethyl ether (1.05g).

Synthesis of 5-(4-isothiocyanatophenyl)-l0,15,20-triphenylporphyrine (TPP-ITC)

A mixture of TPP-NH_2 (61 mg, 0.1 mmol) and *N,N'*-thiocarbonyldipyridone (46 mg, 0.2 mmol) in dichloromethane (20 mL) was stirred at room temperature under argon for 2 h. Dichloromethane (DCM) was removed by evaporation and the residue was chromatographed on a silica column with a 50/50 petroleum ether /DCM mixture. The compound was precipitated with petroleum ether and isolated as a purple powder (57 mg, 85%) ^{1}H NMR (300 MHz, $CDCl_3$) δ (ppm): 8.91 (AB system, J = 4.8 Hz, 2H), 8.89 (s, 4H), 8.82 (AB system, J = 4.8 Hz, 2H), 8.25 (m, 8H), 7.82 (m, 9H), 7.67 (d, J = 8.2 Hz, 2H), 2.75 (s, 2H)[22].

Synthesis of fluorescent organic nanoparticles conjugated with tetraphenylporphyrine (FONPs[TPP])

11.5 mg of **FONPs** and 1.5 mg of the **TPP-ITC** (2.2 μM) were dissolved in DMSO (1 mL) and the reaction mixture was heated at 80°C for 16 hours. After addition of DCM (60 mL), flocculation occurred. The mixture was centrifuged and the precipitate was washed twice with DCM and dried under vacuum, yielding 11.5 mg of dark-brown powder (26 % with respect to **TPP-ITC**).

Characterization of the FONPs and FONPs[TPP]

Transmission electron microscopy (TEM). The sizes of the **FONPs-[TPP]** were determined by TEM imaging which was carried out on a HITACHI H7650 at 80 KV. Copper grids coated with a carbon membrane were pretreated using the Glow discharge technique. One droplet of the aqueous nanoparticle solution was deposited on the grid; the excess of liquid was gently drawn-off with paper and the sample was further stained with uranyl acetate. The nanoparticles were randomly and manually counted using the ImageJ program (using a circle selection). The diameter of each nanoparticle was measured and the results were given as a medium size (diameter) of the overall counted nanoparticles. For the statistics, 858 nanoparticles were counted.

Zeta potential (ζ). Zeta potential analysis was performed with a SZ-100Z Horiba instrument. Ten measurements were realized for each sample according to a predefined operating procedure and the final values were calculated as an average of the overall measurements.

UV-visible absorption and fluorescence spectroscopies. All photophysical properties were analyzed with freshly prepared air equilibrated solutions at room temperature (293 K). UV/Vis absorption spectra were recorded using a Jasco V-570 spectrophotometer. Steady-state fluorescence measurements were performed on diluted solutions (optical density < 0.1) contained in standard 1 cm quartz cuvettes using a Horiba FluoroMax spectrometer or a Fluorolog spectrometer in photon-counting mode. Fully corrected emission spectra were obtained for each compound at $\lambda_{ex} = \lambda_{abs}^{max}$ with an optical density at $\lambda_{ex} \leq 0.1$ to minimize internal absorption.

Cell culture

BE(2)-M17 cells line (ATCC (CRL-2267)) were cultured in Opti-MEM Reduced-Serum Medium (Invitrogen Cat.#: 31985-088) with 10 % FBS, 1% penicillin-streptomycin (Gibco 15140-122) and 0.5 % G418 (0.5 mL of 100 mg/mL). They were routinely maintained at 37 °C and 5 % CO_2.

Two-photon imaging of the cell internalization of FONPs[TPP] in human cancer cells

BE(2)-M17 cells were seeded for imaging in a 6-well plate. After 8 h, cells were treated with **FONPs-[TPP]** (64 µg/mL) for 16 h at 37 °C. The culture medium was removed and the cells washed twice with PBS before imaging experiments. The cells were imaged using a confocal microscope used a Leica TCS SP5 on an upright stand DM6000 (Leica Microsystems, Mannheim, Germany), equipped with the objective HCX APO L U-V-I 63.0X water NA 0.90. The multiphoton microscopy was performed with a tunable pulsed laser Mai Tai HP (Spectra-Physics, Irvine, USA), tuned at 790 nm (output average power of 2.8 W) or 730 nm (output average power of 2.2 W). Photons were collected by an internal PMT respectively in the 600-770 nm and 400-720 nm wavelength ranges.

Acknowledgements

This study was achieved within the context of the Laboratory of Excellence TRAIL ANR-10-LABX-57. The authors are grateful to Benjamin Dehaye for generous gift of BE(2)-M17 cells and to Franck Couillaud for access to cell culture facilities. We thank Guillaume Clermont for Zeta potential measurements. The fluorescence and electronic microscopies experiments were performed in the Bordeaux Imaging Center, a service unit of the CNRS-INSERM and Bordeaux University, member of the national infrastructure France BioImaging supported by the French National Research Agency (ANR-10-INBS-04). The help of Sabrina Lacomme is acknowledged.

REFERENCES

1. Moghissi K, Dixon K, Gibbins S. *Surg. J.* 2015; **1**: e1–e15.
2. Dąbrowski JM, Arnaut LG.*Photochem. Photobiol. Sci.*, 2015; **14**: 1765-1780.
3. Verlhac JB, Clermont G, Blanchard-Desce M. *J. Porphyrins Phtalocyanines* 2017; **21**: 77-87.
4. Pérez-Herrero E, Fernández-Medarde A. *Eur. J. Pharm. Biopharm*. 2015; **93**: 52-79.
5. Nabil G, Bhise K, Sau S, Atef M, El-Banna HA, Iyer AK. *Drug Discov. Today* 2019; **24**: 462-491.
6. Yingchoncharoen P, Kalinowski DS, and Richardson DR. *Pharmacol. Rev.* 2016; **68**: 701–787.
7. Cabral H, Kataoka K. *J. Control. Release* 2014 ; **190**: 465-476.
8. de Campos VEB, Ricci-Júnior E, Mansur CRE. *J. Nanosci. Nanotechnol*. 2012; **12** :2881-2889.
9. Delplace V, Couvreur P, Nicolas J. *Polym. Chem*., 2014; **5**: 1529–1544.
10. Kaminskas LM, McLeod VM, Porter CJH, Boyd BJ. *Mol. Pharmaceutics* 2012; **9**: 355−373.
11. Kumar A, Zhang,X, Liang, XJ. *Biotechnol. Adv.* 2013; **31**: 593–606.
12. Kong T, Hao L, Wei Y, Cai X, Zhu B. *Cell Proliferation* e12488.
13. Wu DQ, Li ZY, Li C, Fan JJ, Lu B, Chang C, Cheng SX, Zhang XZ, Zhuo RX. *Pharmaceutical Research.* 2010; **27**: 187-199.

14. Cespedes MV, Unzueta U, Tatkiewicz W, Sanchez-Chardi A, Conchillo-Sole O, Alamo P, Xu Z, Casanova I, Corchero JL, Pesarrodona,M, Cedano J, Daura X , Ratera I, Veciana J, Ferrer-Miralles N, Vazquez E, Villaverde A, Mangues R. *ACS Nano* 2014; **8**: 4166-4176.
15. Wei G, Wang Y, Huang X, Hou H, Zhou S. *Small Methods* 2018, 21700358.
16. Swierczewska M, Han HS, K. Kim K, Park JH, Lee S. *Adv. Drug Deliv. Rev.*2016; **99**: 70-84.
17. Sofias AM, Dunne M, Storm G, Allen C. *Adv. Drug Deliv. Rev.* 2017; **122:** 20-30.
18. Daniel J, Montaleytang M, Nagarajan S, Picard S, Clermont G, Lazar AN, Dumas N, Correard F, Braguer D, Blanchard-Desce M, Estève MA, Vaultier M. *ACS Omega* submitted
19. Hammerer F, Poyer F, Fourmois L, Chen. S, Garcia G, Teulade-Fichou MP, Maillard P, Mahuteau-Betzerab F. *Bioorg. Med. Chem.* 2018; **26**: 107-118.
20. Makarov NS, Drobizhev M, Rebane A. *Optics Express* 2008; **16**:4029-4047.
21. Starkey JR, Rebane AK,.Drobizhev MA,Meng F, Gong A, Elliott A, McInnerney K and.Spangler CW. *Clin Cancer Res* 2008; **14**: 6564-6573.
22. Tasan S, C. Licona, Doulain PE, Michelin C, Gros CP, Le Gendre P, Harvey PD, Paul C, Gaiddon C, Bodio E. *J. Biol. Inorg. Chem*. 2015; **20**: 143-154.

Figure and scheme captions

Table 1. Fluorescence properties of **FONPs**, **FONPs[TPP]** in water. For comparison purpose, data for **TPP** in toluene are also given.

Scheme 1. Synthetic pathway for the preparation of **FONPs[TPP]**. Step 1: synthesis of the fluorescent organic nanoparticles (**FONPs**); step 2: activation to (**FONPs-NH_2**); step 3: conjugation with 5-(4-isothiocyanatophenyl)-l0,15,20-triphenylporphyrine (**TPP-ITC**).

Fig.1. A: TEM images of **FONPs-NH_2**; B: Size distribution of **FONPs-NH_2** fitted with a log normal; C: TEM images of **FONPs[TPP]**; D: Size distribution of **FONPs[TPP]** fitted with a log normal.

Fig. 2. Absorption spectra of the **FONPs** (dotted line) and of the **FONPs[TPP]**(solid line) with inset showing the Q-bands.

Fig. 3. Emission and excitation spectra of the **FONPs[TPP]**. A: emission spectra (dotted line, λ_{ex} = 360 nm and solid line, λ_{ex} = 520 nm); B: excitation spectra (dotted line, λ_{em} = 450 nm and solid line, λ_{em} = 650 nm)

Fig. 4. Two-photon fluorescence imaging of BE(2)-M17 cells incubated with **FONPs[TPP]**. A: Bright field; B: Two-photon fluorescence upon excitation at 790 nm, the fluorescence is collected in the 600-770 nm wavelength range (inset: corresponding emission spectrum recorded in the cells); C: overlap of the bright field and the two-photon fluorescence imaging.

Fig. 5. Two-photon fluorescence imaging of BE(2)-M17 cells incubated with **FONPs[TPP]**. A: Bright field; B: Two-photon fluorescence upon excitation at 730 nm, the fluorescence is collected in the 450-550 nm wavelength range; C: overlap of the bright field and the two-photon fluorescence imaging.

Table 1. Fluorescence properties of **FONPs**, **FONPs[TPP]** in water. For comparison purpose, data for **TPP** in toluene are also given.

Compound	λ_{abs}^{max} (nm)	$\lambda_{\alpha bs}^{max}$ (Q bands, nm)	λ_{exc}^{max} (nm)	λ_{em}^{max} (nm)	Φ_f
TPP	420	516, 550, 594, 650		654, 722	0.11[a] [3]
FONPs	360	-		460	0.13[b]
FONPs[TPP]	360, 420	520, 555, 590, 650	360 520	460 655,720	0.05[b] 0.03[c]

[a)] in toluene, fluorescence quantum yield determined relative to cresyl violet in methanol (Φ_f= 0.54)
[b)] fluorescence quantum yield determined relative to quinine sulfate in 1N H_2SO_4 (Φ_f = 0.546)
[c)] fluorescence quantum yield determined relative to **TPP** in toluene.

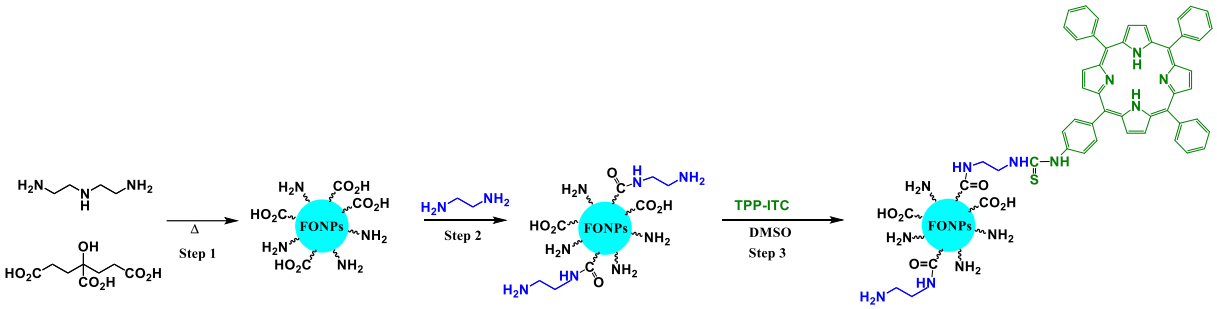

Scheme 1. Synthetic pathway for the preparation of **FONPs[TPP]**. Step 1: synthesis of the fluorescent organic nanoparticles (**FONPs**); step 2: activation to (**FONPs-NH_2**); step 3: conjugation with 5-(4-isothiocyanatophenyl)-l0,15,20-triphenylporphyrine (**TPP-ITC**).

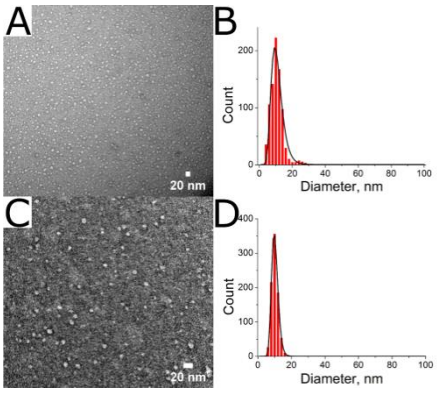

Fig.1. A: TEM images of **FONPs-NH_2**; B: Size distribution of **FONPs-NH_2** fitted with a log normal; C: TEM images of **FONPs[TPP]**; D: Size distribution of **FONPs[TPP]** fitted with a log normal.

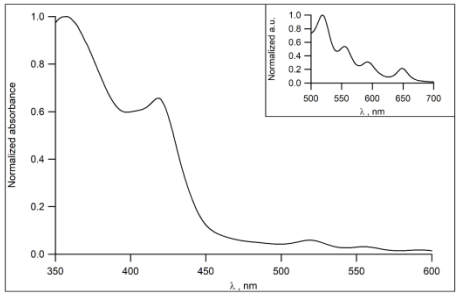

Fig. 2. Absorption spectra of the **FONPs** (dotted line) and of the **FONPs[TPP]** (solid line) with inset showing the Q-bands.

A

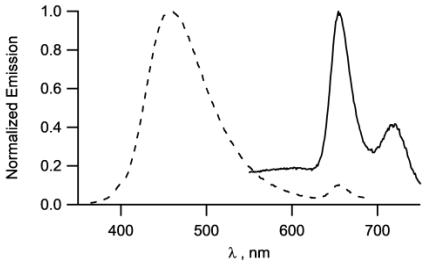

B

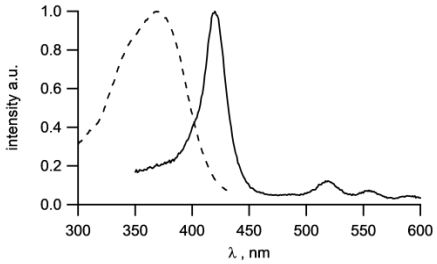

Fig. 3. Emission and excitation spectra of the **FONPs[TPP]**. A: emission spectra (dotted line, λ_{ex} = 360 nm and solid line, λ_{ex} = 520 nm); B: excitation spectra (dotted line, λ_{em} = 450 nm and solid line, λ_{em} = 650 nm)

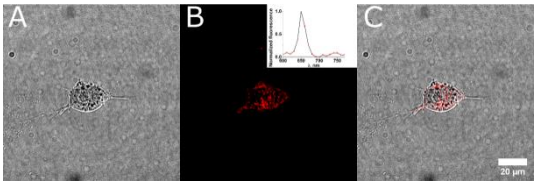

Fig. 4. Two-photon fluorescence imaging of BE(2)-M17 cells incubated with **FONPs[TPP]**. A: Bright field; B: Two-photon fluorescence upon excitation at 790 nm, the fluorescence is collected in the 600-770 nm wavelength range (inset: corresponding emission spectrum recorded in the cells); C: overlap of the bright field and the two-photon fluorescence imaging.

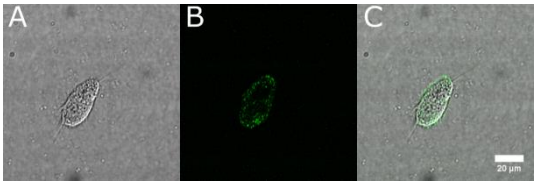

Fig. 5. Two-photon fluorescence imaging of BE(2)-M17 cells incubated with **FONPs[TPP]**. A: Bright field; B: Two-photon fluorescence upon excitation at 730 nm, the fluorescence is collected in the 450-550 nm wavelength range; C: overlap of the bright field and the two-photon fluorescence imaging.

Soft fluorescent organic nanodots as nanocarriers for porphyrins

Isabelle Sasaki, Jonathan Daniel, Sébastien Marais, Jean-Baptiste Verlhac, Michel Vaultier and Mireille Blanchard-Desce

The synthesis of new highly water-soluble fluorescent organic nanoparticles functionalized with hydrophobic tetraphenylporphyrin (TPP) was achieved. The conjugated nanoparticles show two distinct fluorescences, which arise from the nanocarrier (blue fluorescence) and from the linked porphyrin (red fluorescence), depending on the excitation wavelengths. Thanks to this property, we could observe the uptake of the conjugated nanoparticles into neuroblastoma cancer cells by two-photon microscopy.